



# Infrared Spectra and Interstellar Sulfur: New Laboratory Results for H<sub>2</sub>S and Four Malodorous Thiol Ices

Reggie L. Hudson and Perry A. Gerakines

Astrochemistry Laboratory, NASA Goddard Space Flight Center, Greenbelt, MD 20771, USA; [Reggie.Hudson@NASA.gov](mailto:Reggie.Hudson@NASA.gov)  
Received 2017 October 28; revised 2018 September 24; accepted 2018 September 26; published 2018 November 9

## Abstract

New infrared spectra are presented for H<sub>2</sub>S and four other sulfur-containing compounds, all thiols, at 10–140 K to aid in the study of interstellar and solar system ices. Infrared spectral changes on warming H<sub>2</sub>S and each thiol are described with an emphasis on the S–H stretching vibration at 2550–2525 cm<sup>-1</sup> ( $\lambda = 3.92\text{--}3.96\ \mu\text{m}$ ) as it is in a relatively unobscured part of the infrared spectra of interstellar and planetary ices. Infrared positions and band strengths for each thiol's S–H and C–H stretching vibrations are reported, along with the S–H band strength of H<sub>2</sub>S. Two band strengths of near-infrared features of CH<sub>3</sub>SH are included. Results for these compounds are compared, and some areas of agreement and disagreement with the literature are described.

*Key words:* astrobiology – astrochemistry – infrared: ISM – ISM: molecules – molecular data

## 1. Introduction

The abundance of sulfur in the dense interstellar medium (ISM) is a long-standing problem in astrochemistry. Abundances of sulfur-containing molecules and ions are about as expected for diffuse interstellar clouds, but are low by a factor of as much as a thousand for dense molecular clouds (Prasad & Huntress 1982; Anderson et al. 2013). A possible explanation is that the missing sulfur is present in the icy mantles that coat interstellar dust grains, but relatively few infrared (IR) spectra of candidate sulfur ions or molecules have been studied at relevant ice temperatures and even fewer such spectra have been accompanied by IR band strengths.

In addition to an interstellar presence, several sulfur-containing molecules, such as H<sub>2</sub>S, SO<sub>2</sub>, and OCS, have been identified in cometary comae, and CH<sub>3</sub>SH and CH<sub>3</sub>CH<sub>2</sub>SH have been identified at the nucleus of Comet 67P/Churyumov–Gerasimenko with the *Rosetta* lander's mass spectrometer (Altwegg et al. 2017). Sulfur chemistry also is known to be active in clouds of our solar system's four giant planets, in the atmosphere of Venus, and on several icy moons, such as Europa. Finally, sulfur is one of the main biogenic elements, and a component of the amino acid cysteine found in terrestrial biology.

Laboratory experiments should be able to identify likely candidate sulfurous molecules for astronomical study, but at present there is a dearth of baseline data to guide such work. Therefore, in this paper we report new laboratory results for H<sub>2</sub>S and four organic sulfur-containing molecules known as thiols, traditionally abbreviated as RSH where R represents a hydrocarbon group. Thiols are the sulfur equivalents of alcohols (ROH), but unlike alcohols they have received relatively little study by laboratory astrochemists. Here we present new results for solid thiols, specifically those where R is –CH<sub>3</sub>, –CH<sub>2</sub>CH<sub>3</sub>, –CH<sub>2</sub>CH<sub>2</sub>CH<sub>3</sub>, and –CH(CH<sub>3</sub>)<sub>2</sub>, the methyl, ethyl, 1-propyl, and 2-propyl groups, respectively. Our goal is to provide new data to better guide and support future laboratory and telescopic programs, as well as space-based observations involving sulfur-containing molecules.

## 2. Experimental Methods

Our earlier papers should be consulted for details of our preparation of ice samples and our measurements of IR spectra, IR band strengths ( $A'$ ), and refractive indices ( $n_{\text{vis}}$ ), and the use of interference fringes to measure ice thicknesses; see, for example, Gerakines & Hudson (2015a, 2015b). Briefly, ice samples were prepared by vapor-phase deposition onto a pre-cooled KBr substrate within a vacuum chamber interfaced to an FTIR spectrometer. The deposition rates used gave increases in sample thicknesses between 1 and 4  $\mu\text{m}$  per hour. No dependence of our results on deposition rate between these limits was found. IR spectra were recorded as 100-scan accumulations at 2 cm<sup>-1</sup> resolution unless otherwise specified. Hydrogen sulfide (H<sub>2</sub>S) gas was purchased from Matheson. All four thiol reagents were liquids, were purchased from Sigma Aldrich, and were used as received aside from simple drying and freeze–pump–thaw degassing.

Refractive indices were needed to measure ice thicknesses, and densities ( $\rho$ ) were needed to derive IR band strengths (Hollenberg & Dows 1961). The density and reference refractive index of H<sub>2</sub>S used will be treated in the next section. For our four amorphous thiol ices, we used  $n_{\text{vis}} = 1.42$  and  $\rho = 0.888\ \text{g cm}^{-3}$ , based on our results with CH<sub>3</sub>SH (Hudson 2016), since the liquid-phase  $n_{\text{vis}}$  and  $\rho$  values for these compounds are essentially identical. The wavelength used for  $n_{\text{vis}}$  measurements was 670 nm.

The equation used to calculate IR apparent band strengths ( $A'$ ) is

$$A' = \left( \frac{2M}{N_{\text{fringes}} \lambda_{\text{laser}} N_A} \right) \left( \frac{n_{\text{vis}}}{\rho} \right) \times \int_{\text{band}} (\text{Absorbance}) d\tilde{\nu} \quad (1) \quad (2.303)$$

where  $M$  is the sample's molar mass ( $\text{g mol}^{-1}$ ),  $N_{\text{fringes}}$  is the number of interference fringes measured during the sample's deposition,  $\lambda_{\text{laser}}$  is the wavelength (670 nm) of the laser used to record the fringes,  $N_A$  is Avogadro's number, and the integration is over the IR band of interest. Such  $A'$  values are needed to determine molecular abundances in

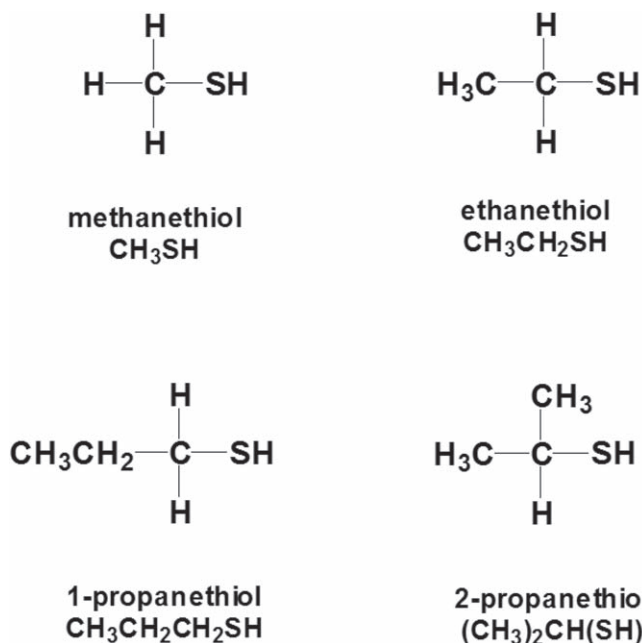


**Figure 1.** Names and line structures of the four organic compounds studied.

interstellar ices using astronomical spectra (Gerakines & Hudson 2015a, 2015b).

Note that in Equation (1) two compound-specific constants,  $n_{\text{vis}}$  and  $\rho$ , are needed to determine  $A'$ , and that the uncertainty in  $A'$  depends primarily on the uncertainties in  $n_{\text{vis}}$  and  $\rho$ . We estimate that  $n_{\text{vis}}$  is good to within  $\pm 0.01$ , or about 1%, but  $\rho$  could be off by 10%, making the latter our best estimate for an uncertainty in  $A'$ . See our recent papers for more on this topic (e.g., Hudson et al. 2017).

We caution that all five of the sulfur compounds we investigated are not only detrimental to laboratory equipment, but they also are volatile, toxic, and accompanied by an “intolerable foetor” (Lavoisier 1789), which no doubt has limited their study. Appropriate safeguards are urged in working with them.

### 3. Results

Our new results will be presented by first considering  $\text{H}_2\text{S}$  and then each of the four thiols studied, followed by an examination of some trends in the data. Figure 1 gives the names and line structures for the organosulfur compounds investigated.

#### 3.1. $\text{H}_2\text{S}$ Results

Hydrogen sulfide,  $\text{H}_2\text{S}$ , is the simplest closed-shell compound with an S–H bond. It has long been known to be an interstellar molecule (Thaddeus et al. 1972) and recently has been found in a protoplanetary disk (Phoung et al. 2018). Within the solar system,  $\text{H}_2\text{S}$  is a cometary species (Bockelée-Morvan et al. 1991) and has been reported to be an ice in the atmosphere of Uranus (Irwin et al. 2018).

IR spectra of solid  $\text{H}_2\text{S}$  have been studied for at least 60 years (Reding & Hornig 1957), with Fathe et al. (2006) reporting results for multiple solid phases. The main spectral feature of interest here is a pronounced S–H stretching feature of  $\text{H}_2\text{S}$  near  $2548\text{ cm}^{-1}$  ( $3.92\text{ }\mu\text{m}$ ), as seen in Figure 2. It has

the same shape as the thiol IR bands we recorded (see below), but is shifted upwards by about  $17\text{ cm}^{-1}$  from them.

Quantitative descriptions of the IR spectrum of amorphous  $\text{H}_2\text{S}$  are surprisingly scarce as shown by tracing the origin of the currently used  $A'(\text{S–H})$  band strength. A recent astrochemical paper on sulfur chemistry (Chen et al. 2015) used  $A'(\text{S–H}) = 2.0 \times 10^{-17}\text{ cm molecule}^{-1}$  for amorphous  $\text{H}_2\text{S}$  at 14 K, taken from a paper of Jiménez-Escobar & Muñoz Caro (2011). The latter authors derived this value by rescaling one from Smith (1991) of  $A'(\text{S–H}) = 2.9 \times 10^{-17}\text{ cm molecule}^{-1}$  for crystalline  $\text{H}_2\text{S}$  at 88 K to amorphous  $\text{H}_2\text{S}$  at 10 K. Smith, in turn, derived his  $A'$  for amorphous  $\text{H}_2\text{S}$  by combining all of the band intensities of Ferraro et al. (1980) for crystalline  $\text{H}_2\text{S}$  in the S–H stretching region. However, it seems to have gone unnoticed for nearly 40 years that these last authors stated neither a refractive index ( $n_{\text{vis}}$ ) nor a density ( $\rho$ ) for their crystalline  $\text{H}_2\text{S}$ , yet our Equation (1) shows that both numbers are needed for band strength determination. This lack of  $n_{\text{vis}}$  and  $\rho$  makes it impossible to independently verify the earlier work and raises questions about the  $A'(\text{S–H}) = 2.0 \times 10^{-17}\text{ cm molecule}^{-1}$  value now used for amorphous  $\text{H}_2\text{S}$ .

Given this situation, we have carried out measurements and estimates related to  $A'(\text{S–H})$  for  $\text{H}_2\text{S}$ . Knowing that substitution of oxygen with sulfur on going from  $\text{CH}_3\text{OH}$  to  $\text{CH}_3\text{SH}$  causes  $n_{\text{vis}}$  to rise by about 0.09 (Hudson 2016), we expected that a similar increase would be found on going from  $\text{H}_2\text{O}$  ( $\sim 1.3$ ) to  $\text{H}_2\text{S}$ . This expectation was met as three determinations gave  $n_{\text{vis}} = 1.41 \pm 0.01$  for amorphous  $\text{H}_2\text{S}$  at 16 K. We know of no direct measurements of density for amorphous  $\text{H}_2\text{S}$ , but again arguments from analogy are useful. The increase in  $\rho$  on going from  $\text{CH}_3\text{OH}$  to  $\text{H}_2\text{O}$  is about  $0.2\text{ g cm}^{-3}$ , so a similar change from  $\text{CH}_3\text{SH}$  to  $\text{H}_2\text{S}$  should give  $\rho \approx 1.1\text{ g cm}^{-3}$  for amorphous  $\text{H}_2\text{S}$ . (This estimate agrees with a Lorentz–Lorentz calculation using our  $n_{\text{vis}} = 1.41$  for solid  $\text{H}_2\text{S}$  and  $n_{\text{vis}} = 1.374$  (Weast 1980) and  $\rho \approx 1\text{ g cm}^{-3}$  (Steele et al. 1906) for liquid  $\text{H}_2\text{S}$ .) With  $n_{\text{vis}}$  and  $\rho$  in hand, we then carried out  $\text{H}_2\text{S}$  depositions for different ice thicknesses. The changes in S–H band areas with thickness for amorphous  $\text{H}_2\text{S}$  at 16 K gave  $A'(\text{S–H}) = 1.12 \times 10^{-17}\text{ cm molecule}^{-1}$  based on five measurements. To our knowledge, this is the first direct determination of  $A'(\text{S–H})$  with  $n_{\text{vis}}$  and  $\rho$  values stated explicitly. Additional work is needed, particularly a density measurement for amorphous  $\text{H}_2\text{S}$ .

#### 3.2. Methanethiol, $\text{CH}_3\text{SH}$

Our previous thiol work was limited to the simplest member of the family,  $\text{CH}_3\text{SH}$ , known both as methanethiol and methyl mercaptan. Amorphous  $\text{CH}_3\text{SH}$  ices were made by slow vapor-phase deposition of  $\text{CH}_3\text{SH}$  gas onto a KBr substrate pre-cooled to 17 K. A survey spectrum of the resulting ice’s C–H and S–H stretching regions is shown as the bottom trace in Figure 3. The most relevant feature for the present paper is the broad S–H band near  $2535\text{ cm}^{-1}$ , which has an apparent band strength of  $A' = 5.41 \times 10^{-18}\text{ cm molecule}^{-1}$  (Hudson 2016).

Crystallization occurred on warming amorphous  $\text{CH}_3\text{SH}$  to about 65 K and holding it there overnight or simply by warming to a slightly higher temperature. However, the resulting ice was often a mixture of the two crystalline forms of  $\text{CH}_3\text{SH}$ , designated  $\alpha$  and  $\beta$ , one form ( $\beta$ ) being the kinetic product of crystallization and the other ( $\alpha$ ) being the thermodynamic product. The transition temperature for the  $\alpha$  and  $\beta$  phases of  $\text{CH}_3\text{SH}$  is 138 K (Russell et al. 1942), well

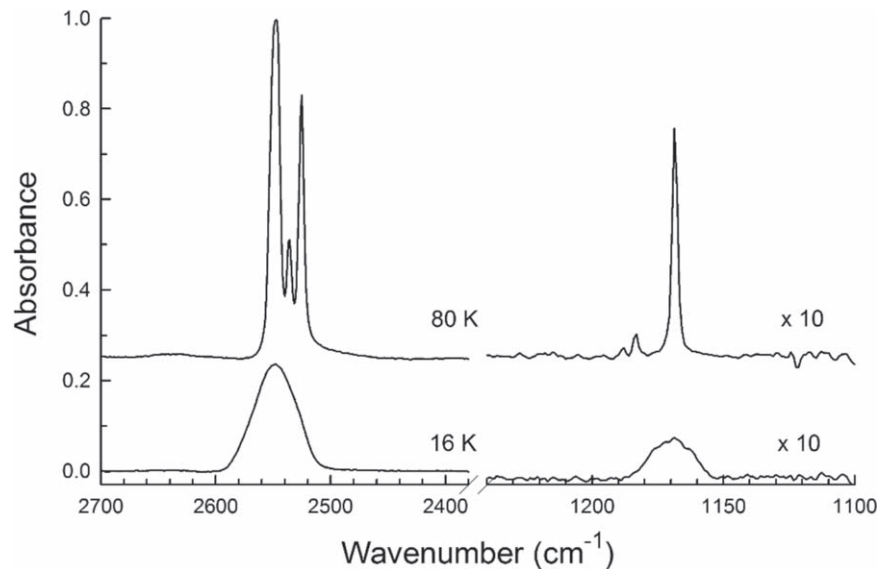


**Figure 2.** Stretching (left) and bending (right) regions of the IR spectrum of amorphous (lower) and crystalline (upper) H<sub>2</sub>S. The ice's thickness was about 4  $\mu\text{m}$ .

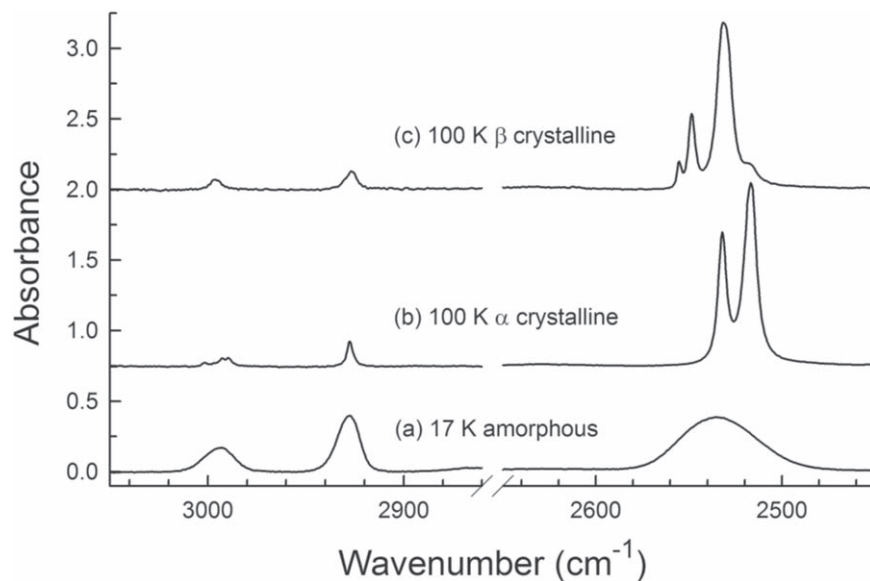


**Figure 3.** C–H (left) and S–H (right) stretching regions of the IR spectra of solid CH<sub>3</sub>SH at 17 K for the amorphous phase and at 100 K for the  $\alpha$ - and  $\beta$ -crystalline phases. The thickness of the amorphous ice was about 7  $\mu\text{m}$ . See Hudson (2016) for details of crystalline CH<sub>3</sub>SH band strengths. Spectra are offset vertically for clarity.

above the  $\sim 120$  K at which CH<sub>3</sub>SH sublimates in our vacuum system. This necessitated somewhat different methods for preparing samples made of just one crystalline phase. See Hudson (2016) for details of the two procedures used.

Although the crystalline forms of CH<sub>3</sub>SH and other thiols are interesting, we view their study in the present context mainly as a way to characterize and recognize them in case they are met while studying amorphous ices in the laboratory. Aside from the low temperatures of dense interstellar clouds, interstellar thiols are expected to have small abundances that will hinder the formation of thiol crystals. However, for reference purposes we also show IR spectra of  $\alpha$ - and  $\beta$ -crystalline CH<sub>3</sub>SH in Figure 3. Tables of CH<sub>3</sub>SH peak positions and band strengths are available for the entire mid-IR region (May & Pace 1969; Hudson 2016).

### 3.3. Ethanethiol, CH<sub>3</sub>CH<sub>2</sub>SH

Following the same procedure used with CH<sub>3</sub>SH, vapor-phase deposition of CH<sub>3</sub>CH<sub>2</sub>SH onto a pre-cooled substrate (16 K) gave an amorphous solid. Warming this ice to 100 K initiated its crystallization, which appeared to be complete after only a few minutes at 110 K. Comparisons of our IR spectra of amorphous and crystalline ethanethiol to those of Smith et al. (1968) showed acceptable agreement in terms of peak positions, shapes, and relative intensities. Calorimetric measurements revealed that only one crystalline phase of CH<sub>3</sub>CH<sub>2</sub>SH exists from  $\sim 14$  to 125 K, the compound's melting point (McCullough et al. 1952), and only one was seen in our work. At 125 K our CH<sub>3</sub>CH<sub>2</sub>SH ices underwent a combination of sublimation and melting, and were quickly lost from the substrate. This behavior resembles that of the related compound CH<sub>3</sub>CH<sub>2</sub>OH (Hudson 2017).

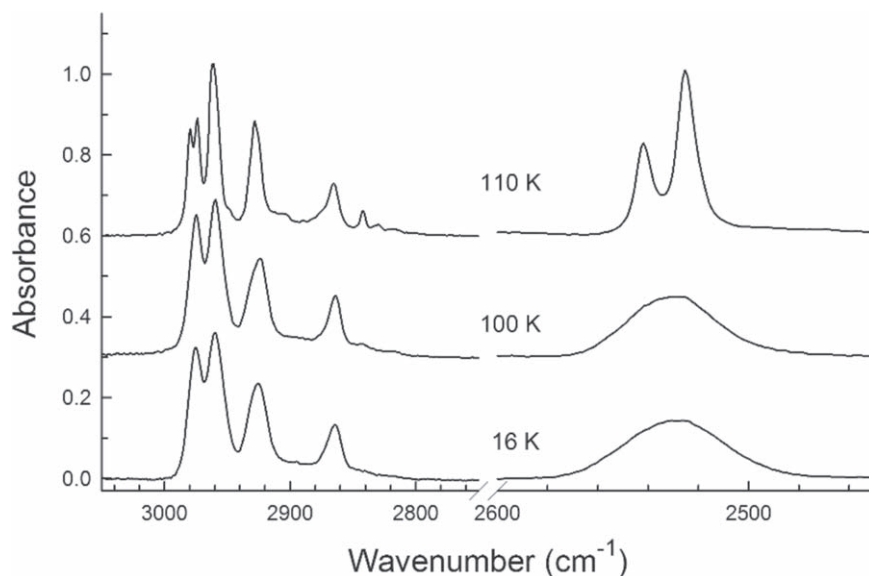


**Figure 4.** C–H (left) and S–H (right) stretching regions of the IR spectra of solid  $\text{CH}_3\text{CH}_2\text{SH}$  deposited at 16 K and warmed to 100 and 110 K. The sample’s original thickness was about  $4.4 \mu\text{m}$ . Spectra are offset vertically for clarity.

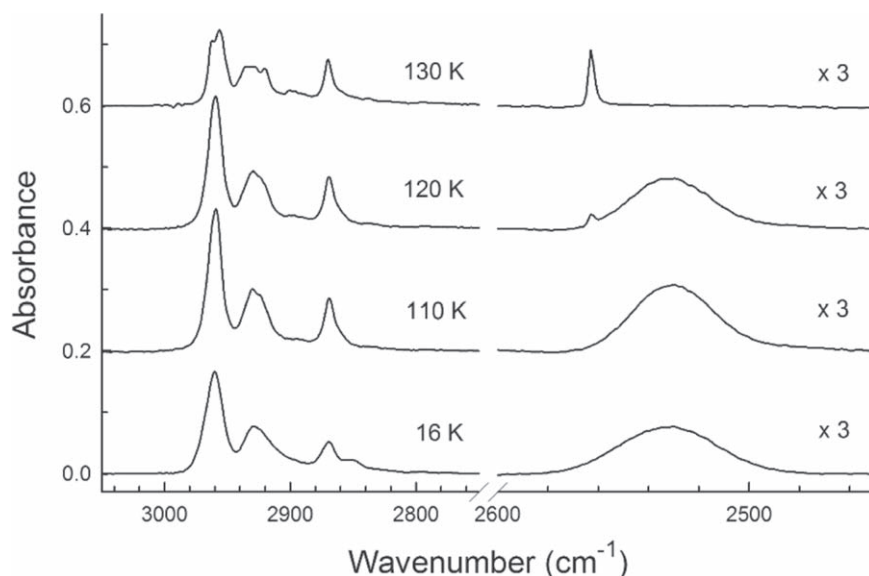


**Figure 5.** C–H and S–H stretching regions of the IR spectrum of solid  $\text{CH}_3\text{CH}_2\text{CH}_2\text{SH}$  deposited at 16 K and warmed to 110, 120, and 130 K. The sample’s original thickness was about  $4.5 \mu\text{m}$ . Spectra are offset vertically for clarity and the right-hand side has been expanded by a factor of 3 (vertically).

Figure 4 shows the C–H and S–H stretching regions of the IR spectra of amorphous and crystalline  $\text{CH}_3\text{CH}_2\text{SH}$ . Note that the conversion on going from the bottom spectrum to the middle one to the top one, corresponding to the amorphous  $\rightarrow$  crystalline change, was irreversible, as are all such crystallizations we have studied.

### 3.4. 1-Propanethiol, $\text{CH}_3\text{CH}_2\text{CH}_2\text{SH}$

Moving from  $\text{CH}_3\text{SH}$  to  $\text{CH}_3\text{CH}_2\text{SH}$  to  $\text{CH}_3\text{CH}_2\text{CH}_2\text{SH}$  one increasingly encounters molecular structures that differ only by rotation around a C–C bond in the molecule. Such individual structures are variously called conformers, conformations, and conformational isomers. As an amorphous ice is warmed, the less stable such conformers can reorient to adopt a more stable form, which is manifested by the disappearance of some IR spectral features and the strengthening of others. We found

little evidence of such effects with  $\text{CH}_3\text{CH}_2\text{SH}$ , but with  $\text{CH}_3\text{CH}_2\text{CH}_2\text{SH}$  several such changes were seen as amorphous 1-propanethiol was warmed from  $\sim 16$  K to about 120 K, at which point our ices began to crystallize. We did not study conformational changes in 1-propanethiol as they already are well known in the literature (e.g., Hayashi et al. 1966; Torgriksen & Klaeboe 1970) and are seen mainly at smaller wavenumbers (longer wavelengths) than those on which we focused.

Figure 5 shows the IR spectrum of 1-propanethiol’s C–H and S–H stretching regions for several temperatures. The rounded shape of the S–H feature in the lower spectrum is indicative of an amorphous ice prepared as already described by deposition near 16 K. The ice began to crystallize on warming to 120 K, as shown by the appearance of a sharp peak at  $2563 \text{ cm}^{-1}$ . Either holding at 120 K or warming to 130 K gave fully crystalline  $\text{CH}_3\text{CH}_2\text{CH}_2\text{SH}$ , whose spectrum is the uppermost in the

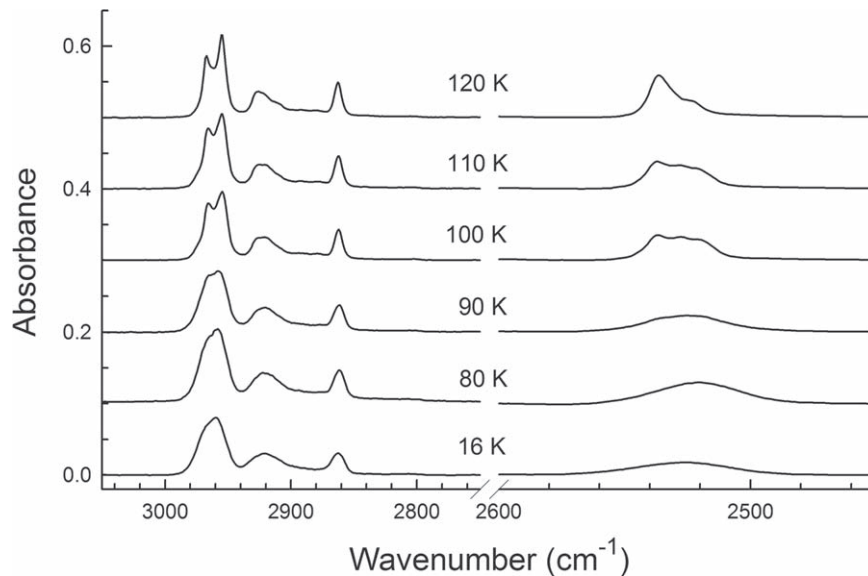


**Figure 6.** C–H and S–H stretching regions of the IR spectra of solid  $(\text{CH}_3)_2\text{CH}(\text{SH})$  deposited at 16 K and then warmed to the temperatures indicated. The sample’s original thickness was about  $4.5 \mu\text{m}$ . Spectra are offset vertically for clarity.

**Table 1**  
IR Band Strengths for Amorphous  $\text{H}_2\text{S}$  and Four Amorphous Thiol Ices at 10–20 K

Compound	Region	Peak Positions ( $\text{cm}^{-1}$ )	Integration Range ( $\text{cm}^{-1}$ )	$A'$ ( $\text{cm molecule}^{-1}$ )
hydrogen sulfide ( $\text{H}_2\text{S}$ )	S–H	2548	2600–2450	$1.12 \times 10^{-17}$
methanethiol ( $\text{CH}_3\text{SH}$ )	C–H	2993, 2928	3020–2900	$2.53 \times 10^{-18}$
	S–H	2535	2600–2450	$5.41 \times 10^{-18}$
				Ratio = 0.47
ethanethiol ( $\text{CH}_3\text{CH}_2\text{SH}$ )	C–H	2975, 2960, 2925, 2864	3020–2800	$1.15 \times 10^{-17}$
	S–H	2528	2600–2450	$4.20 \times 10^{-18}$
				Ratio = 2.74
1-propanethiol ( $\text{CH}_3\text{CH}_2\text{CH}_2\text{SH}$ )	C–H	2960, 2929, 2869	3020–2800	$1.81 \times 10^{-17}$
	S–H	2531	2600–2450	$3.40 \times 10^{-18}$
				Ratio = 5.33
2-propanethiol ( $(\text{CH}_3)_2\text{CH}(\text{SH})$ )	C–H	2960, 2921, 2863	3020–2800	$1.53 \times 10^{-17}$
	S–H	2526	2600–2450	$3.53 \times 10^{-18}$
				Ratio = 4.34

figure. Additional warming resulted in the ice’s complete sublimation at  $\sim 140$  K.

Calorimetric measurements have shown that 1-propanethiol has a crystalline–crystalline transition near 142 K (Pennington et al. 1956), above this compound’s sublimation temperature in our vacuum system. It might have been possible, using a thicker ice and faster scanning, to have rapidly warmed 1-propanethiol above 140 K and then to record the spectrum of the high-temperature crystalline phase before it was lost by sublimation. Alternatively, rapid deposition of 1-propanethiol at 130–140 K could have released enough energy to crystallize the ice into the high-temperature phase, which might have been locked in by a subsequent rapid cooling. We did not pursue either option. It would be interesting to determine if 1-propanethiol adopts an orientationally disordered (plastically crystalline) form for its high-temperature crystalline phase, with an accompanying decrease in the sharpness of its IR features.

### 3.5. 2-Propanethiol, $(\text{CH}_3)_2\text{CH}(\text{SH})$

Figure 6 shows IR spectra for the C–H and S–H stretching regions of 2-propanethiol at several ice temperatures. On

depositing 2-propanethiol in the usual manner near 16 K, an amorphous ice was formed. Warming to 90–100 K caused significant changes in several IR bands, suggesting crystallization. A second change occurred at 110–120 K, suggesting a crystalline–crystalline transition, in agreement with calorimetric measurements on 2-propanethiol showing such a change at 112.5 K (McCullough et al. 1954). However, it was not entirely clear that at 120 K only one crystalline phase was present in our ices. Additional warming did not clarify the situation as our 2-propanethiol ices rapidly sublimated above 130 K.

The paper of Smith et al. (1968) has IR spectra for an amorphous (glassy) form and two crystalline phases of 2-propanethiol, but temperatures were not specified, no thickness information was provided, and the spectra were on a small scale. However, to the extent that comparisons are possible, our work agrees with theirs.

### 3.6. Comparisons and Trends

By the usual methods (Hollenberg & Dows 1961; Gerakines & Hudson 2015a, 2015b), band strengths ( $A'$ ) can be determined for every IR feature of  $\text{H}_2\text{S}$  and each of our thiols

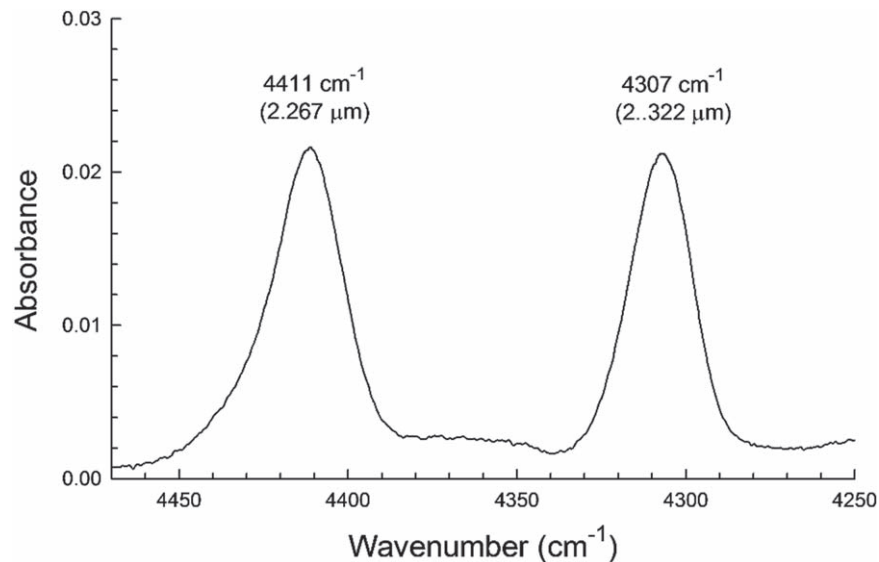


**Figure 7.** Two near-IR bands of amorphous  $\text{CH}_3\text{SH}$  deposited at 10 K. The sample's thickness was about  $3.8 \mu\text{m}$ .

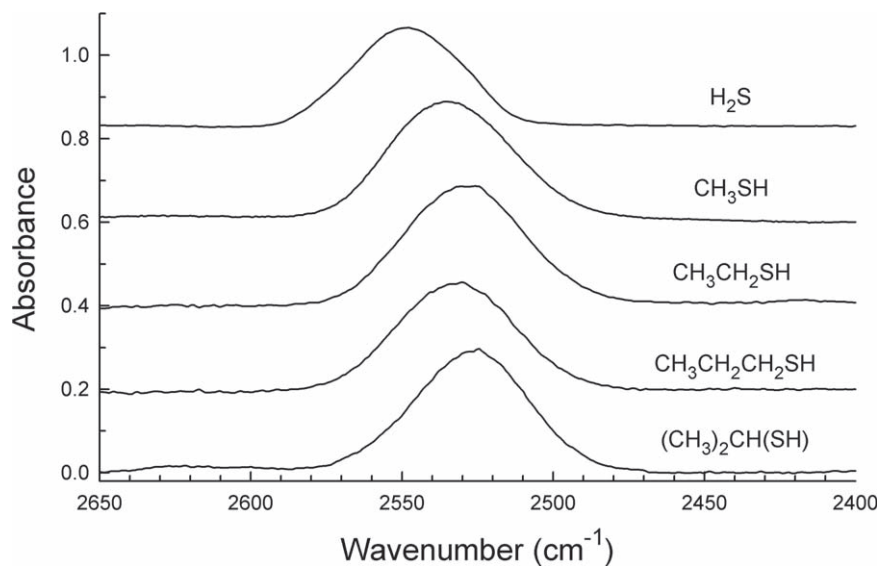


**Figure 8.** IR S–H stretching feature of amorphous  $\text{H}_2\text{S}$  and four amorphous thiols at 10–16 K. Spectra have been scaled to be about the same height.

at multiple temperatures. However, we were mainly interested in each compound's S–H stretching feature near  $2530 \text{ cm}^{-1}$  ( $3.95 \mu\text{m}$ ), and so in Table 1 we have tabulated  $A'$  values for it for each amorphous compound. The corresponding  $A'$  values for the C–H stretching region for each thiol also are included. It is readily seen that  $A'(\text{SH})$  varies little for these four thiols.

The numbers in Table 1 also allow, by appropriate scaling and comparisons, band strengths to be calculated for other IR features of each compound. For example, two near-IR combination bands are shown in Figure 7 for  $\text{CH}_3\text{SH}$ . By comparing their areas to those of the  $\text{CH}_3\text{SH}$  bands in Table 1, we calculated  $A'(4411 \text{ cm}^{-1}, 2.267 \mu\text{m}) = 3.1 \times 10^{-19} \text{ cm molecule}^{-1}$  and  $A'(4307 \text{ cm}^{-1}, 2.322 \mu\text{m}) = 2.4 \times 10^{-19} \text{ cm molecule}^{-1}$ .

A more qualitative, visual comparison of our results is shown in Figure 8, which places the IR spectra of  $\text{H}_2\text{S}$  and our amorphous thiols on a single plot, each spectrum having been recorded at 10–20 K and scaled to give the same peak height. For the thiols, small variations among these four IR bands can be found, but the similarities are far more obvious, such as that

the S–H band of each has a full width at half-maximum of  $44\text{--}49 \text{ cm}^{-1}$ . Note also from Figures 3–6 and our earlier work (Hudson 2016) that the positions and shapes of the S–H bands shown in Figure 8 for our amorphous thiols hardly change with temperature until a phase transition occurs.

## 4. Discussion

### 4.1. Thiol Infrared Spectra and Band Intensities

In the spectra of  $\text{H}_2\text{S}$  and the four thiols we studied, the most likely IR feature for astronomical detection and identification is the S–H stretch near  $2530 \text{ cm}^{-1}$  ( $3.95 \mu\text{m}$ ). Interstellar ices have no other strong IR bands in this region, which is between an intense  $\text{CO}_2$  feature and a strong, broad band of amorphous  $\text{H}_2\text{O}$  ice. However, Figure 8 shows that the IR positions of the S–H features of our five compounds are sufficiently close, and sufficiently similar, that a firm identification of any particular one on spectroscopic grounds alone could be difficult. More positively, that these compounds absorb in the same IR region

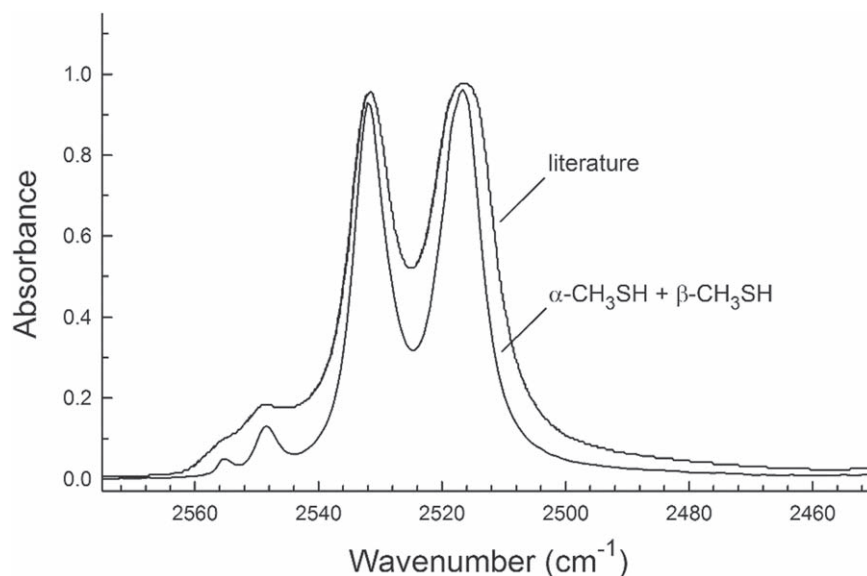


**Figure 9.** Comparison of a recently published IR spectrum of crystalline  $\text{CH}_3\text{SH}$  (Pavithraa et al. 2017b) to a combination of our spectra of the  $\alpha$ - and  $\beta$ -crystalline phases of  $\text{CH}_3\text{SH}$  (Hudson 2016). The fractional contributions are about  $\alpha = 0.55$  and  $\beta = 0.45$ .

suggests that their collective absorbance might produce a detectable feature in an interstellar ice’s spectrum.

A trend seen in Table 1 is that the larger the R group in a thiol, the smaller the intensity of the S–H feature relative to that of the C–H absorptions. This is not so much from the band strength of the thiol S–H group getting smaller, as it is the rise in  $A'$  for the C–H region that makes the S–H feature appear to weaken on going from Figures 3–6. Put differently, the lack of an IR observation of a thiol cannot necessarily be attributed to a particularly small intrinsic band strength, but rather it is more likely due to a low abundance (column density) or overlap with other IR features.

We also found that  $\text{H}_2\text{S}$  and all of our thiols sublimated under vacuum at 100–140 K, well below the 160 K or so at which  $\text{H}_2\text{O}$ -ice sublimates. This means that there is little chance that  $\text{H}_2\text{S}$  and these same thiols can be left behind in a pure crystalline form after  $\text{H}_2\text{O}$  ice sublimation occurs.

#### 4.2. Comparisons to Recent Work

We have already cited numerous papers that relate to the present study, but they are mainly from the older literature. Two recent publications that are close to our work are those of Pavithraa et al. (2017a, 2017b) on ethanethiol and 1-propanethiol respectively. Since those papers did not include ice thicknesses or band intensities, it is impossible to make quantitative comparisons to our results. On a qualitative level most of the IR spectra reported by those authors are similar to ours, but there are at least two points of disagreement.

First, in describing our  $\text{CH}_3\text{SH}$  work the authors (Pavithraa et al. 2017b) state that “the molecule (sic) was found to exist in three solid phases, which depends on the temperature and thickness of the icy layer (Hudson 2016).” However, no claim for such a thickness dependence was made in our paper and none has been found during the present work. We know of no evidence for a phase change with thickness for any of our thiols.

Second, two of the three IR spectra in those same authors’ Figure 5 (Pavithraa et al. 2017b) are not for a single crystalline phase, but rather are from a mixture of two forms of ice. Their

spectrum of crystalline 1-propanethiol is actually from a partially crystallized amorphous ice as shown by the simultaneous presence of both a sharp and a broad S–H IR feature, indicating amorphous and crystalline components, respectively. Similarly, those authors’  $\text{CH}_3\text{SH}$  spectrum is actually for an ice made of two distinct phases. Our Figure 9 shows that their  $\text{CH}_3\text{SH}$  spectrum (digitized from the literature) can be fitted with a combination of our spectra of  $\alpha$ - $\text{CH}_3\text{SH}$  and  $\beta$ - $\text{CH}_3\text{SH}$ . Note that our spectra are of a slightly higher resolution ( $1\text{ cm}^{-1}$ ) to better define the various IR features.

#### 4.3. Applications

The primary connection of our work to astronomical and astrochemical research is that we have generated a self-consistent set of IR spectra of  $\text{H}_2\text{S}$  and four thiol ices, each accompanied by band strengths, apparently measured for the first time. The latter can be used to estimate upper limits of abundances in interstellar ices or, in the event of an observation of an S–H band, calculating an abundance (column density). These same  $A'$  values allow one to determine band strengths for IR features we have not studied, and which might lie in unobscured spectral regions. For planetary observers, we have characterized two near-IR features for  $\text{CH}_3\text{SH}$  in this way, which could be useful for observations of Kuiper Belt objects and satellites of the outer solar system.

The extent to which our results contribute to solving the missing interstellar sulfur problem remains to be seen. What can be said with confidence is that our new results show that (i) the S–H IR features of  $\text{H}_2\text{S}$  and simple organosulfur compounds do not possess unusually low IR band strengths and (ii) they do not suffer extensive overlap with spectra of such strong absorbers as  $\text{H}_2\text{O}$  ice, frozen  $\text{CO}_2$ , or silicates. The *James Webb Space Telescope*’s high sensitivity and speed may be able to both detect and resolve  $\text{H}_2\text{S}$  and thiols, depending on their abundances. Multiple reports have appeared concerning gas-phase interstellar  $\text{CH}_3\text{SH}$  and at least one paper has been published (Kolesniková et al. 2014) for gas-phase interstellar  $\text{CH}_3\text{CH}_2\text{SH}$ , raising the possibility that our work can help to shed light on these two molecules in the ISM.

Our work also provides a significant basis for further laboratory investigations. For example, spectra such as we have presented could be used to calculate IR optical constants, a task we have completed for several nitriles and hydrocarbons (e.g., Moore et al. 2010; Hudson et al. 2014a, 2014b). The response of the S–H stretching band to the presence of H<sub>2</sub>O ice should be investigated, although our experience with H<sub>2</sub>S suggests that the changes will be small (Moore et al. 2007). Our  $A'$  values could be used to measure vapor pressures by the method of Khanna et al. (1990), and there might even be sufficient vapor-pressure differences to drive enrichments of the heavier thiols in ices. Finally, we have yet to explore reaction chemistry involving thiols in icy environments, either thermal chemistry, radiation chemistry, or photochemistry. It would be interesting to determine some of the more likely reactions that these malodorous materials undergo under extraterrestrial conditions.

### 5. Conclusions

This paper has presented both qualitative and quantitative results for H<sub>2</sub>S and four thiols. Each compound has a well defined S–H stretching band in the 2550–2525 cm<sup>-1</sup> ( $\lambda = 3.92\text{--}3.96\ \mu\text{m}$ ) region, which is otherwise relatively unobscured for spectral observations of interstellar and planetary ices. IR band strengths have been measured for all five compounds to aid in the study of abundances and to assist in lab-to-lab comparisons. The thiol S–H band's intensity has been found to be roughly constant and somewhat smaller than that of H<sub>2</sub>S.

Support from NASA's Astrophysics Research and Analysis (APRA) program is acknowledged as is support from the NASA Astrobiology Institute through funding awarded to the Goddard Center for Astrobiology under proposal 13-13NAI7-0032.

### ORCID iDs

Reggie L. Hudson  <https://orcid.org/0000-0003-0519-9429>

Perry A. Gerakines  <https://orcid.org/0000-0002-9667-5904>

### References

- Altwegg, K., Balsiger, H., Berthelier, J. J., et al. 2017, *MNRAS*, **469**, S130
- Anderson, D. E., Bergin, E. A., Maret, S., & Wakelam, V. 2013, *ApJ*, **779**, 141
- Bockelée-Morvan, D., Colom, P., Crovisier, J., Despois, D., & Paubert, G. 1991, *Natur*, **350**, 318
- Chen, Y.-J., Juang, K.-J., Nuevo, M., et al. 2015, *A&A*, **798**, 80
- Fathe, K., Holt, J. S., Oxley, S. P., & Pursell, C. J. 2006, *JPCA*, **110**, 10793
- Ferraro, J. R., Sill, G., & Fink, U. 1980, *AcSpA*, **34**, 525
- Gerakines, P. A., & Hudson, R. L. 2015a, *ApJL*, **805**, L20
- Gerakines, P. A., & Hudson, R. L. 2015b, *ApJL*, **808**, L40
- Hayashi, M., Shiro, Y., & Murata, H. 1966, *Bull. Chem. Soc. Japan*, **39**, 112
- Hollenberg, J., & Dows, D. A. 1961, *JChPh*, **34**, 1061
- Hudson, R. L. 2016, *PCCP*, **18**, 25756
- Hudson, R. L. 2017, *AcSpe*, **187**, 82
- Hudson, R. L., Ferrante, R. F., & Moore, M. H. 2014a, *Icar*, **228**, 276
- Hudson, R. L., Gerakines, P. A., & Moore, M. H. 2014b, *Icar*, **243**, 148
- Hudson, R. L., Loeffler, M. J., & Gerakines, P. A. 2017, *JChPh*, **146**, 0243304
- Irwin, P. G. J., Toledo, D., Garland, R., et al. 2018, *NatAs*, **2**, 420
- Jiménez-Escobar, A., & Muñoz Caro, G. M. 2011, *A&A*, **536**, A91
- Khanna, R. K., Allen, J. E., Jr, Masterson, C. M., & Zhao, G. 1990, *J. Phys. Chem.*, **94**, 440
- Kolesníková, L., Tercero, B., Cernicharo, J., et al. 2014, *ApJL*, **784**, L7
- Lavoisier, A. 1789, *Traité Élémentaire de Chimie* (Paris: Cuchet) [Translated by R. Kerr as *Elements of Chemistry in a New Systematic Order Containing All the Modern Discoveries*, 1790]
- May, I. W., & Pace, E. L. 1969, *AcSpA*, **25**, 1903
- McCullough, J. P., Finke, H. L., Scott, D. W., et al. 1954, *JACS*, **76**, 4796
- McCullough, J. P., Scott, D. W., Finke, H. L., et al. 1952, *JACS*, **74**, 2801
- Moore, M. H., Ferrante, R. F., Moore, W. J., & Hudson, R. L. 2010, *ApJS*, **191**, 96
- Moore, M. H., Hudson, R. L., & Carlson, R. W. 2007, *Icar*, **189**, 409
- Pavithraa, S., Methikkalam, R. R. J., Gorai, P., et al. 2017a, *AcSpA*, **178**, 166
- Pavithraa, S., Sahu, D., Seth, G., et al. 2017b, *ApSS*, **362**, 126
- Pennington, R. E., Scott, D. W., Finke, H. L., et al. 1956, *JACS*, **78**, 3266
- Phoung, N. T., Chapillon, E., Majumdar, L., et al. 2018, *A&A*, **616**, L5
- Prasad, S. S., & Huntress, W. T., Jr. 1982, *ApJ*, **260**, 590
- Reding, F. P., & Hornig, D. F. 1957, *JChPh*, **27**, 1024
- Russell, H., Jr., Osborne, D. W., & Yost, D. M. 1942, *JACS*, **64**, 165
- Smith, D., Devlin, J. P., & Scott, D. W. 1968, *JMoSp*, **25**, 174
- Smith, R. G. 1991, *MNRAS*, **249**, 172
- Steele, B. D., McIntosh, D., & Archibald, E. H. 1906, *RSPTA*, **205**, 99
- Thaddeus, P., Kutner, M. L., Penzias, A. A., Wilson, R. W., & Jefferts, K. B. 1972, *ApJL*, **176**, L73
- Torgrimsen, T., & Klæboe, P. 1970, *Acta. Chem. Scan.*, **24**, 1149
- Weast, R. C. 1980, *CRC Handbook of Chemistry and Physics* (61st ed.; Boca Raton, FL: CRC Press)